GEOPHYSICS, VOL. 72, NO. 2 (MARCH-APRIL 2007); P. F57–F64, 8 FIGS.
10.1190/1.2435081

Multichannel, full waveform and flexible electrode combination resistivity-imaging system

Jingping Zhe[1], Stewart Greenhalgh[1], and Laurent Marescot[2]

ABSTRACT

The development of a new multichannel and multielectrode, full waveform resistivity acquisition system is presented. This system, which can be built in any electronics workshop without major difficulties, allows for large data collection capacity and flexibility but without the sacrifice of channels, as in most other systems that use a preselected array. A superior interpretation quality is enabled by the increased data and the monitoring of noise through full waveform display. The proposed hardware is robust because no electronics need to be installed in the cable. Therefore, it is suitable for 2D or 3D surface or crosshole tomography. A major feature of the data collection strategy is to capture all of the electrode combinations subject to having one current electrode in each cable. This is efficient because there is no extra cost in doing this. It is an automatic process; one does not have to make any prior decisions as to what electrode combinations to use. The data sets collected with this strategy are suitable for an inversion process involving a large amount of data because the number of voltage values measured using a couple of current electrodes is maximized. Synthetic modeling shows that the proposed approach allows for better imaging of the subsurface than with conventional arrays and the results are comparable to results obtained with an optimized experimental design strategy. A field experiment illustrates the effectiveness of the presented strategy. The inverted image of the subsurface is well-correlated with the available borehole information.

INTRODUCTION

Relative simplicity, low equipment cost, and ease of use combine to make direct current (DC) resistivity imaging a useful and increasingly popular subsurface exploration technique in civil engineering, hydrology, and environmental investigations (Meekes, 1993; Chambers et al., 1999; Ogilvy et al., 1999; Slater et al., 2000; Marescot et al., 2004). Resistivity surveys are used to locate groundwater, determine depth to bedrock, assess soil characteristics, or determine seepage paths in earth dams. Resistivity techniques can also be used to detect groundwater pollution and contamination; estimate hydraulic parameters; and characterize fractures, cavities, saltwater intrusions, waste dumps, or contaminant plumes. Earth resistivity imaging is also being applied in mining and archaeology. Surveys are increasingly being carried out in built-up areas where electrical noise is high, which makes resistivity measurements challenging.

Traditionally, 2D resistivity imaging data are collected as a combination of sounding and profiling using well-defined electrode configurations, such as Wenner, Schlumberger, dipole-dipole, pole-dipole, and pole-pole. The choice of arrays stems from various historical and technical considerations. In the past, this was mainly a way to methodically build an apparent resistivity pseudosection as a means of display and preliminary interpretation and to identify any gaps in the coverage of a profile. It was also recognized that the response of the subsurface to galvanic currents is highly dependent on the electrode array used. Dahlin and Zhou (2004) undertook a numerical comparison of the 2D resistivity imaging capabilities of ten popular surface electrode arrays. They studied five synthetic geological models of relevance to civil engineering projects to assess effectiveness (anomaly effects, signal-to-noise ratio) and imaging acuity (resolution) of these ten arrays. They show that the particular choice of a predefined array depends largely on the site conditions, field logistics, and the type of survey target. This could encourage real-time experimental design, such as the approach proposed by Stummer et al. (2004), although this technique is presently highly time-consuming and not supported by common hardware.

We suggest a break from the usual practice of imaging with a particular array. Rather, one should take as many measurements as practical from a fixed set of electrodes and record from numerous combinations of current and potential electrodes. Such an approach is dependent on having fast, computer-controlled, multichannel data acquisition, preferably of the full voltage waveform. Recent devel-

Manuscript received by the Editor March 27, 2006; revised manuscript received September 15, 2006; published online February 9, 2007.
[1]University of Adelaide, Department of Physics, Adelaide, South Australia. E-mail: jingping.zhe@adelaide.edu.au; stewart.greenhalgh@adelaide.edu.au.
[2]Swiss Federal Institute of Technology, Institute of Geophysics, Zürich, Switzerland. E-mail: laurent@aug.ig.erdw.ethz.ch.

opments in multielectrode cables, fast switching, and digital recording, combined with availability of powerful 3D modeling and inversion codes, make it timely to advocate such an approach to resistivity imaging.

CONVENTIONAL 2D AND 3D RESISTIVITY IMAGING

In 2D surface resistivity imaging, voltages are measured for various electrode spacings at horizontal locations along the ground surface to yield a 2D picture of vertical and horizontal resistivity variations in the subsurface. Reliable and efficient data collection based on multiple electrodes, typically 48, 96, or 128, and on daisy-chained multicore cables and junction boxes have been available for some time for surface array scanning using pole-pole, pole-dipole, Wenner, dipole-dipole, and other common configurations (e.g., Barker, 1981; Griffiths et al., 1990; Xu and Noel, 1993; Beresnev et al., 2002). Inversion codes used to translate the raw voltage measurements into 2D resistivity models are also available (Tripp et al., 1984; Li and Oldenburg, 1992; Loke and Barker, 1996a; Loke and Dahlin, 2002).

Crosshole resitivity surveying, in which the source electrodes and the potential electrodes are placed downhole in two horizontally separated boreholes and moved over a range of depths, is able to yield detailed information on the variation of electrical conductivity between the boreholes (Daniels, 1977, 1983). Tomographic inversion procedures for crosshole 2D imaging have been developed by various people (Daily and Owen, 1991; Shima, 1992; Zhou and Greenhalgh, 1999, 2000, 2002). In crosshole surveys, the pole-pole array is often used. Zhou and Greenhalgh (2000) numerically analyzed the sensitivity patterns and anomaly amplitudes for a variety of crosshole electrode configurations and concluded that the bipole-bipole and pole-bipole arrays performed best.

Whereas 3D inversion codes already exist (Park and Van, 1991; Sasaki, 1992; Zhang et al., 1995; Loke and Barker, 1996b), the use of 3D resistivity imaging, either for distributions of surface electrodes or for multiple borehole arrays, has been limited until now by the large computational expense required for the inversion of 3D data sets within a reasonable time. Another problem is the time-consuming data acquisition when using single-channel, multielectrode arrays.

In practice, the pole-pole array is frequently used in the field to increase the spatial resolution of data sets, especially near the grid boundaries in 3D (Park and Van, 1991; Li and Oldenburg, 1992; Dahlin and Bernstone, 1997). This array needs one remote electrode which has to be placed a long distance away from the working site to meet the theoretical assumptions. The pole-pole array is susceptible to noise in populated areas because the data can be contaminated by stray voltages from electric sources (e.g., power lines, leakage currents) along the wires connecting the remote electrodes. This prompts one to use other electrode arrays, such as pole-dipole or dipole-dipole. This not only reduces the disturbance of random noise outside the working site but makes it possible to concentrate the current flow through the region of interest. The pole-dipole configuration has a better resolution than the pole-pole array (Sasaki, 1992). The major disadvantages of dipole-dipole arrays are the low signal strength when the distance between the dipoles is increased and poor data coverage near the edges of the grid when using only axial dipole-dipole configurations.

The foregoing discussion highlights the limitations of standard electrode arrays for 2D and 3D electric imaging. The other limiting factor is the limited number of independent recording channels and the difficult measurement conditions in boreholes.

RESISTIVITY INSTRUMENTATION

Commonly used systems

The basic components for a resistivity system are a DC power supply (100 V to 2000 V), ammeter, cable, electrodes, and a high-impedance voltmeter. One of the first papers to deal with multielectrode systems was that of Barker (1981). Others include Griffiths et al. (1990), Meju and Montague (1996), Beresnev et al. (2002) and Stummer et al. (2002, 2004). Current focusing, important in certain situations like borehole measurements, is discussed by Jackson (1981), Roy and Dutta (1997), Kampke (1999), and others.

There are a number of available multielectrode resistivity systems for shallow surveying, such as the Syscal (Iris Instruments), SuperSting R8 (AGI Inc), Tomoplex (Campus Ltd), SAS 4000 Lund (ABEM), GeoTom (Geolog), RESECS (DMT GmbH), and the GMS 150 (GeosSys). An exhaustive comparison is given by Stummer et al. (2004). The number of electrodes is typically in the range 30 to 256, but most units are single-channel and most record from each electrode in a serial fashion. Single-channel recording can be extremely time-consuming. Some instruments, such as the Syscal Pro, SuperSting R8, and the RESECS, offer more channels (10, 8, and 8, respectively) but do not record full waveforms (only averaged values) and are usually used with one of the standard electrode configurations. Effective recording for these standard arrays is often achieved by sacrificing several channels. Dahlin and Zhou (2006) proposed the gradient array for a more efficient 2D resistivity imaging using existing multichannel devices.

Distributed data acquisition for real-time experimental design

Stummer et al. (2002) developed a new distributed data acquisition resistivity system in which waveforms are digitized and partially processed at each electrode before being transmitted to a central computer for storage, further processing, display, and interpretation. They built a 100-channel version in which each digital acquisition unit (DAU) can be configured as a current source, current sink, voltage reference, or measuring device. Such parallel recording vastly speeds up survey operations. They were motivated by real-time experimental design, which entails a number of data acquisition-data analysis cycles that are, presently, highly time consuming. Stummer et al. (2004) did not record the maximum of possible combinations but used data sets that contain the most important information, recorded in an optimization sense. Their system is versatile but limited in overall length by voltage drops across the digital data bus. It is also expensive, with a separate DAU at each electrode, and somewhat cumbersome to handle. For example, this system could be difficult to use in boreholes. Also, the time to perform a data download of the entire waveforms is quite lengthy when the number of recorded data is large. Nevertheless, significant improvements should be certainly achieved in the future to make this approach really attractive.

New concept in resistivity recording

We adopted an alternative approach of having a single, centralized multichannel data acquisition unit, which operates on a similar principle to a computer network. Analog voltage signals from the

various electrodes are transmitted through multicore cables to the central unit. A built-in switch matrix allows arbitrary pairs of electrodes to inject currents into the ground and arbitrary potential electrode configurations. The voltage signals pass through a multiplexer before being fed to a single analog-to-digital converter. Parallel recording is thus achieved by means of multiplexing in the same way that digital seismographs operate. A single box includes most of the electronics, so only a single instrument has to be stored and operated. By having relatively few electrical connections between system components, the possibility of leakage currents is reduced and overall reliability is increased. Cost is much less than for a distributed system. As our system is centralized, no delicate components are present on the cables. The cables can have simple takeouts (or exposed metal electrodes) at some preassigned interval, such as 5 m, and can be laid out on the ground surface. They are then connected to metal electrodes driven into the ground by means of short wires terminated at either end with an alligator clip. Alternatively, the cables can be simply lowered down a borehole where galvanic contact with the ground is achieved by having the takeouts in direct contact with the borehole fluid. To meet the requirements of such a new concept in resistivity recording, a more versatile/flexible way of collecting the data must be devised. These aspects are addressed in the following section.

A PROTOTYPE SYSTEM

A prototype resistivity acquisition and inversion system, to test the concepts of automation, multichannel full waveform recording, and versatile/flexible electrode combination, was recently designed and built by us. Our primary aim in building this system was proof of concept, and to provide a tool for use by university researchers in both laboratory and field resistivity experiments. In the following sections we provide a brief description of the system hardware and software, point out the essential design features, and explain how it can be used in various survey situations.

Recording hardware

We give here a more detailed description of the proposed resistivity acquisition strategy. The description, although specific to the prototype, is also somewhat generic, and similar systems can be fabricated in electronics workshops elsewhere without major difficulties. Our home-built, prototype system can simultaneously measure one current pair and 26 potentials (27 channels). In this paper, the system is presently limited to 27 channels, although many more channels are possible (e.g., a 64-channel version is under development) depending on the needs of the user. In its present configuration, the prototype system uses two multicore cables, each of which has 14 in-built electrodes acting as either current or voltage probes. Figure 1 shows the basic recorder in its carrying case. The junction box on the left mates through multipin connectors to the two multielectrode cables. It allows individual electrode selection. This box is, in turn, connected to the controlling/recording PC (not shown) and to the power/control box on the right. Figure 2 presents a block diagram of the control box showing the basic interconnections. This box performs high-speed multiplexing and A/D conversion (resolution 16 bits, with an input voltage range ±5 V), and permits simultaneous multichannel acquisition. Each of the 26 voltage channels is sampled every 1.25 ms, and the samples are averaged over a 16-sample window to provide one effective (averaged) sample every 20-ms sampling per channel. This helps eliminate 50-Hz power-line interference by summing over a full cycle of 16 samples (20 ms). The in-built filter to automatically reject 50-Hz noise during acquisition makes the prototype system suitable for use in built-up areas. The multiplexer, of course, operates at a much faster rate to enable sampling of all channels and processing in less than 1.25 ms. The power converter box is used to provide the input current waveform. It draws its power from a 12-V car battery. There are three voltage output options (75 V, 145 V, and 270 V) and four gain-control functions on recording (1, 2, 4, and 8). The current waveform is a commutated DC signal with adjustable frequency (typically 0.25 to 0.5 Hz), number of cycles (typically 1 or 2), and length of dead time between polarity reversals. With a 4-s period signal, the positive current is applied for 1 s (50 samples), then it is shut off for 1 s (50 samples), the current goes negative for 1 s, and it is shut off for 1 s before the next cycle is repeated (if at all). This would result in recording a 200-sample waveform for each cycle and for each channel. The digital time series are saved onto disc on the PC.

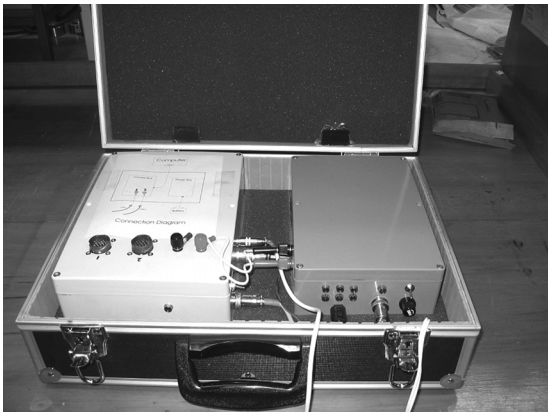

Figure 1. Photograph of the prototype multichannel, full waveform resistivity recording system. The two multielectrode cables connect to the junction box on the left, which is connected to the power/control box on the right and to a PC. The control box performs high-speed multiplexing and A/D conversion.

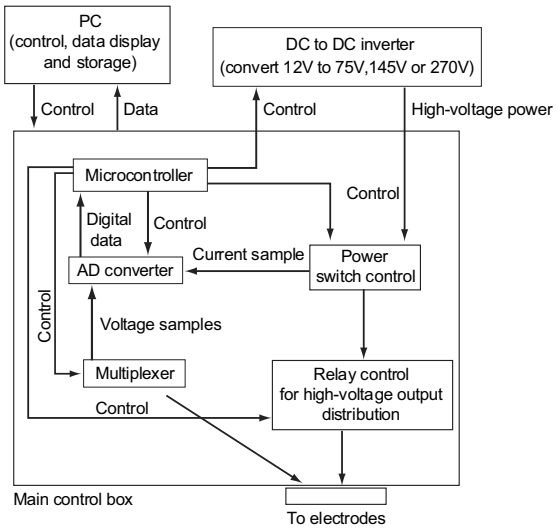

Figure 2. Block diagram of the control box for the new measurement device.

We decided to write special software to control the hardware, to make the visualization of the full-waveform possible, to perform preliminary processing, and to store the data. The survey configuration and parameters (such as electrode positions, output voltage, period of the current waveform, number of cycles, and gain control) are recorded in a control file that controls data acquisition for each experiment. The electrode connections can also be checked prior to data acquisition and the results displayed on screen.

After the survey is completed, apparent resistivities are calculated from the processed voltage waveforms (after averaging values over the flat portions of the reversed waveforms and removing self potentials (SPs), the current values, and the electrode geometry files. These values are then inverted to produce a 2D (or 3D) map of true resistivity variations. The recorded raw time-series potential and current data can be further examined, filtered and reprocessed later with advanced signal processing techniques if required.

Versatile electrode geometry

A particular recording strategy has to be devised for data collection with the new acquisition system. Figure 3 illustrates schematically the layout for a crosshole survey using the presented measurement device. This is the survey configuration for which the flexible prototype system was originally designed, but it can also be used for other survey geometries. Fourteen-electrode cables are placed in each borehole. We normally place a current source in one hole and a current sink in the other to ensure large voltages and to get the current to preferentially flow through the inter-well medium of interest. The electrodes are numbered from 1 to 14 on the diagram. For a given pair of current electrodes (e.g., +I at position 1 in hole 1 and −I at position 7 in hole 2), 26 potentials are simultaneously recorded. A reference potential (e.g., electrode 4) is set for hole 1, and all 13 voltages at positions 2 to 14 in hole 2 (those not occupied by the current sink) are measured relative to this position. Similarly, a reference potential (e.g., electrode 10) is taken in hole 2, and all voltages at positions 2 to 14 in hole 1 (those not occupied by the source) are measured relative to this position. No common ground is required because potential differences are measured.

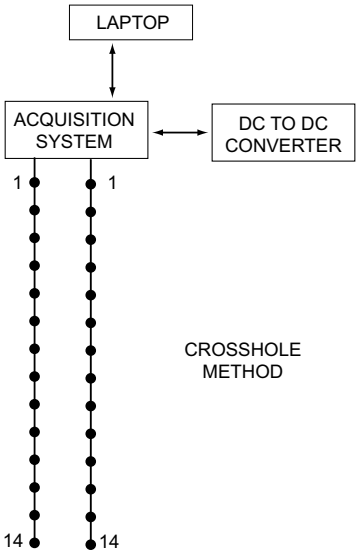

Figure 3. Layout for a crosshole electrical survey. The two 14-electrode cables are placed in two separated boreholes. A current source and sink are established in each hole and 13 voltage differences are simultaneously measured relative to two reference positions, one in each borehole, to yield 26 voltage waveforms for each current bipole. With $14 \times 14 (= 196)$ possible current bipoles, the total number of waveforms recorded with the presented strategy is $196 \times 26 = 5096$.

The choice of reference potential electrodes is not critical. It is simply set in terms of proximity (multiples of electrode spacing) to the current electrode in each cable. In the example above, it is fairly close (three-electrode intervals away) to the current electrode. This is to get a large signal by having at least one potential electrode on each measurement close to a current electrode. But the operator can choose how far away it should be at the time of survey execution. In principle, the separation between the reference electrodes and the current electrodes in each cable can be different for each current pair, but it is normally kept fixed throughout the survey and specified in the control file. In other words, the voltage reference is set relative to the (dynamic) current position. After the first set of 26 potential differences are taken, a new set of current positions are chosen (e.g., source +I at electrode 2 in hole 1 and sink −I at electrode 5 in hole 2). Then, a new set of 26 potentials are recorded relative to the new reference electrodes in each hole, again making sure that only those 13 electrodes in each hole not occupied by a current position are used. For example, the reference electrode in cable 1 may now be at position 5, and that in hole 2, at position 8. There are $14 \times 14 = 196$ possible combinations of the current electrodes using this recording strategy. The total number of voltage waveforms recorded is, therefore, $26 \times 196 = 5096$. A complete survey run takes approximately 16 min. The display of Figure 6 shows the 14 traces in each well for a crosshole survey. The current source is at electrode 1 in well 1, and the current sink is at electrode 2 in well 2. The reference traces are at electrode 3 in well 1 and at electrode 4 in well 2 and show zero volts. The voltage waveform traces next to the current source and sink exhibit the largest excursions. The particular current waveform used (shown at the top left of the picture) and replicated in shape in the voltage waveforms is initially negative, then zero for a short period, and then positive.

The important point to make is that, in the proposed approach, the user can record or recover all possible voltage differences for a given pair of current electrodes. In other words, a reference electrode (e.g., station 3) is set up in cable 1, and all voltages are recorded for all electrodes in cable 2 relative to this point. A reference electrode is then set up in cable 2 (e.g., station 7), and all voltages in cable 1 are recorded relative to this point. Because the voltage difference between electrode 3 in cable 1 and electrode 7 in cable 2 is known (from the first set of 13 measurements), it is possible to deduce (by simple addition and subtraction) all possible voltage differences over and above those directly measured. The only limitation, compared to the comprehensive data set of Stummer et al. (2004), is that the new acquisition strategy does not have a full set of current bipoles because it forces one current electrode to be in each cable. But apart from this restriction, it yields all possible electrode combinations. A system such as we describe does not need multiple analogue-to-digital converters with unique isolated grounds.

Borehole-to-surface (Figure 4) and surface resistivity surveys (Figure 5) can also be readily conducted with this approach. The two obvious cable layouts for the latter are either end-to-end (cable layout 1) or interleaved (cable layout 2) as shown in Figure 5. The current electrodes are placed in separate cables. So, if the cables are placed end-to-end, it is not possible to have the source (A) and sink (B) in the same cable, which seems to mitigate against certain elec-

trode configurations like dipole-dipole or Wenner arrays. But by interlacing the cables, with some slight overlap (say, one-electrode spacing), one can still cover almost the entire line with A (in cable 1) and also with B (in cable 2). So, although it is not possible to exactly embrace standard arrays like Wenner, one can closely approximate them and still get full coverage along the line.

Philosophy of data recording strategy

We give here a discussion on the philosophy behind this way of collecting the data and some differences with respect to the more traditional approaches. In the acquisition strategy described above, all 27 channels are used all of the time, one for current measurement and 26 for potential measurements. There is no option to use just some channels. No decisions need to be made in advance as to which electrode combinations to use, such as with some other instruments. The whole process can be automated and the scheme is efficient because all of the data is captured. The aim is not to optimize survey design by having some prior knowledge of the target. It is not a case of having a limited number of measurements to make and wanting to make the best use of them. Our philosophy is to collect as much data as possible (subject to the restrictions mentioned earlier on current electrode combinations). It does not cost any more time to collect all combinations of electrodes; so, it is not an issue. Our primary emphasis was to develop a fast and efficient field acquisition strategy for data collection which allows maximum flexibility. One can always discard data later, before or during inversion, after examining the voltage levels and the noise. In most cases, one does not know what is best in advance. If the preconceived notion of the subsurface is wrong, then errors can be incurred using standard electrode arrays or optimized survey designs. The subjective judgments of what data to use can be made later (post-survey), in the light of preliminary inversion results. Data can be brought in or dropped, as required. It takes no longer to collect it all, using all channels simultaneously. Whatever restrictions apply to some other data collection systems do not apply here.

Full waveform display and recording

Although not imperative, we strongly recommend, to anyone who wants to build a system like ours, to use a real-time display of the voltage waveforms. In the present example, the survey execution is under software control, and the various combinations required are specified in the input control file. After this control file is loaded, the electrode positions and survey geometry can be displayed on the screen. Real-time display of the voltage waveforms for all 26 channels are displayed as they are acquired to allow the survey progress to be dynamically monitored and the survey run to be interrupted if required (see Figure 6). The current pulse is also displayed. When the waveforms are completed, for as many cycles of forward and reverse polarity as desired, then a new set of current electrodes is chosen, and the potential measurements re-initiated (but for different reference electrodes) and displayed. Any noise spikes, unusual voltage decays, or other anomalous measurements are quickly spotted. The full waveforms are saved and can be inspected later. The main purpose to capture and display waveforms is for survey quality control. Noisy electrodes can be identified, including those showing charge-up effects (if converting from a current to a potential electrode). The display provides reassurance that the voltages are sensible and allows one to immediately appreciate S/N levels. Of course, with the waveform data, it is possible to do subsequent signal enhancement or processing not possible with other instruments. This feature has not yet been fully exploited. Nor has the use of decay characteristics to determine induced polarization (IP) effects. In fact, the system is not optimized for IP recording. The sampling rate is, perhaps, a bit coarse (20 ms per channel) and is made problematic by the 16-sample averaging (at 1.25-ms intervals) that is employed to combat 50-Hz noise. The sampling is more than adequate over the

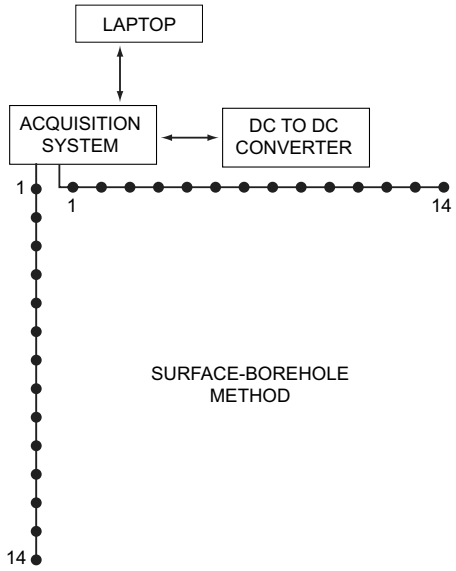

Figure 4. Layout for surface-to-borehole resistivity experiment. One cable of 14 electrodes is laid out on the surface, the other cable is positioned down the borehole. One electrode on each cable is used for current; the other 13 are used for potential measurement. By taking all possible combinations of 14×14 current bipoles and measuring 26 voltages for each (13 from each cable relative to a reference potential on the other cable), 5096 waveforms can be automatically recorded in less than one-half hour.

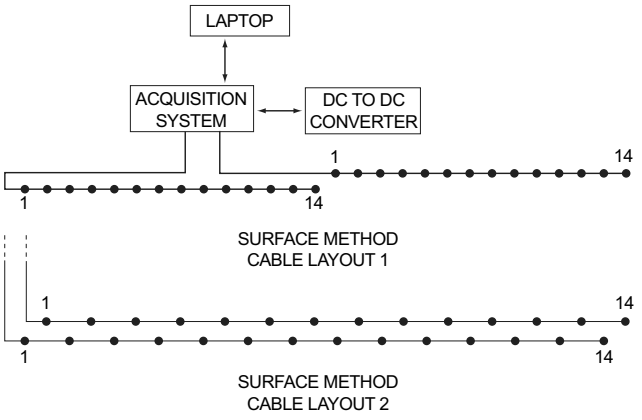

Figure 5. Layout for a surface resistivity survey. The two 14-electrode cables can be either placed end-to-end or interleaved.

major portion of the square waveform but is not fast enough at the pulse edges (switch-on and switch-off times) to capture electromagnetic (EM) and IP effects.

A SYNTHETIC EXAMPLE

A simulation experiment was conducted to compare the performance of the new resistivity survey configuration with that of other electrode arrays. The synthetic data was computed for the model shown in Figure 7a. This is the model adopted by Stummer et al. (2004) to test optimized real-time experimental design systems. The reader is referred to the Stummer et al. (2004) paper for actual inversion results for a variety of electrode configurations. Here, we present our results for the new flexible electrode combination system (~3000 data points) using a damped, least squares and constrained algorithm (see Greenhalgh et al., 2006). The model, shown in diagram A of Figure 7, is essentially a two-layer structure with a lower-resistivity surface layer of thickness 5 m and resistivity 100 ohm-m, overlying a half-space of resistivity 300 ohm-m. The half-space contains two rectangular-shaped anomalies, one a conductor (resistivity grading from 100 to10 ohm-m at the centrer) and the other, a resistor (resistivity 10,000 ohm-m). The conducting body is of size 25×20 m and is buried at a depth of 10 m. The anomalous resistive body is 15 m long and 5 m thick and is located at a depth of 2.5 m. It actually penetrates the overburden. A total of 28 electrodes at 5-m-spacing, extending a distance of 140 m over the top surface of the model were used for the experiment. The Stummer et al. (2004) trials involved 30 electrodes at 5-m-spacing, covering a slightly longer section of line. For the Wenner configuration, only 135 data points were available. For the dipole-dipole array the number of simulated measurements was 147. The combined Wenner-dipole-dipole array used 282 data points. With the new proposed electrode configuration, 5096 data points are collected, but only 3200 data points are used for the inversion. Those having very small voltages are neglected because, with actual field data, such measurements would be captured by noise. The reference electrodes, which vary with each current injection pair, were chosen to be three spacings distant from the actual A and B electrodes in use for each measurement. The inversion result for data obtained with the new configuration is shown in Figure 7b. Both anomalies (conductor and resistor) are well recovered, not only in position and shape, but also in actual resistivity values. The resistivities in the tomogram vary over four orders of magnitude. The Wenner, dipole-dipole, and combined Wenner-dipole-dipole inversions are presented by Stummer et al. (2004). These standard configurations completely fail to recover the low-resistivity anomaly (see Stummer et al., 2004, Figure 1), and produced significant distortion of the resistivity field elsewhere. Even the thickness of the overburden layer is under-estimated. This improvement in the image with the flexible electrode strategy obviously comes from the increase in resolution of the data set. Nevertheless, the most important feature in this example is that, when using a conventional data collection strategy, 116 injection couples need to be recorded with the Wenner array. Only 196 injection couples are necessary to record the 5096 data points with the new resistivity survey configuration. This means that for almost the same number of electrodes and a comparable acquisition time, the information content of a data set can be greatly improved with the new data-collection strategy. Stummer et al. (2004) reached similar conclusions from their synthetic data tests. They compared the resolution obtained on inverted images obtained using a dense electrode combination array (suitable for use with their new distributed data acquisition system). This included five optimized data sets involving 282, 670, 1050, 5740, and 10,310 measurements. Their inversion results (Stummer et al., 2004, Figure 5) for the 5,740 and 10,310 data points are of very similar quality and appearance to that presented here for the new flexible electrode array. Only by using the comprehensive data set of all 51,373 data points were they able to obtain a slightly improved image over ours.

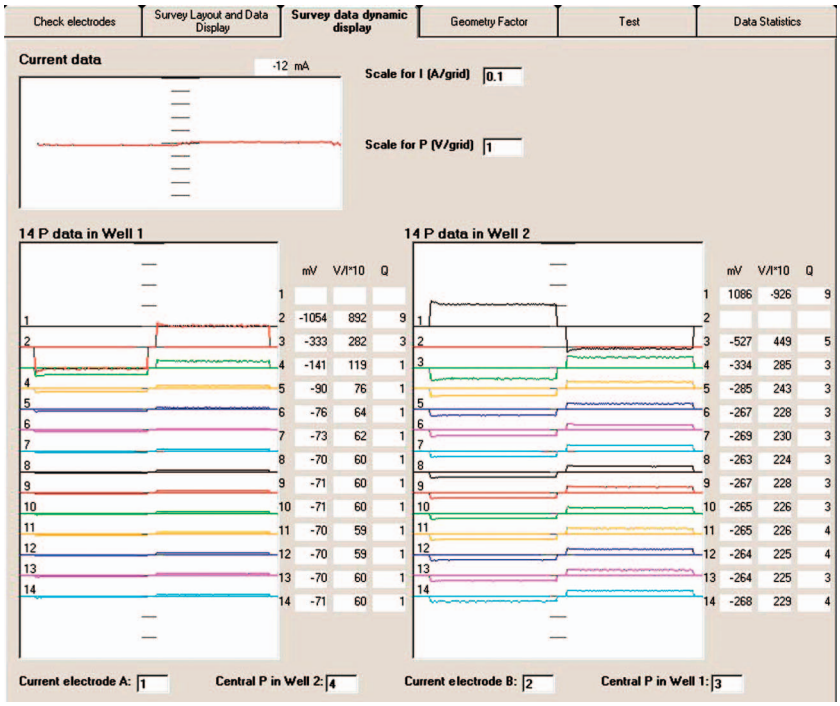

Figure 6. Screen display of the system while a survey is underway. The voltage waveforms from all 26 channels (13 from each cable) are shown in real time, as is the current waveform. The menu also allows for electrode checking; display of survey geometry, which is stored in an input file; and interruption of survey execution.

A FIELD EXAMPLE

As an illustration of the versatility and flexibility of the prototype system, we show the results (Figure 8) from a surface electrical imaging experiment at Coober Pedy, South Australia. The purpose of the survey was to map the shallow subsurface in connection with opal prospecting. The survey was conducted using two 14 electrode cables placed end-to-end at an electrode interval of 6 m. Another infill line was interleaved with the first one, at a 3-m offset, as shown schematically in the diagram. The two lines were merged and processed together to yield a total of 56 electrodes at 3-m-spacing. Again, the reference electrodes are dynamic and selected to always be three spacings away from the active current electrode in each cable. The actual data acquisition took only $2 \times 16 = 32$ min, but the electrode layout took much longer. The surface material is

quite dry; therefore, salt water was needed to reduce contact resistance. The 168-m-long line is fairly flat. In total, 10,182 voltage waveforms were recorded for the various current-potential electrode combinations with the 56 electrodes. A 2.5D resistivity inversion program (Zhou and Greenhalgh, 2000) was used to process the data and produce the 2D true resistivity image shown in Figure 8. The time taken for the inversion was about one hour on a 2.8-GHz, Pentium 4 computer. The geological logs from two drillholes (A03 and A04) are shown superimposed on the image. Basically, the 2- to 4-m-thick top layer comprises mainly alluvium and silty clay with silcrete pebbles. This layer is underlain by a 2- to 6-m-thick layer of silcrete in calcareous silty clay. Next, there is weathered white sandstone, which appears fairly resistive. It grades into a weathered sandstone and then into a conductive mudstone at A04. This basal zone is wet and soft. Fault zones within the sandstone/mudstone are the primary opal targets because of possible ancient water flow through them, although none are known in this particular locality. The resistivity image matches the well logs most favorably, especially the continuous silcrete and white sandstone layer, which is well-imaged. This 8-ohm-m, or less, conductive zone is correlated

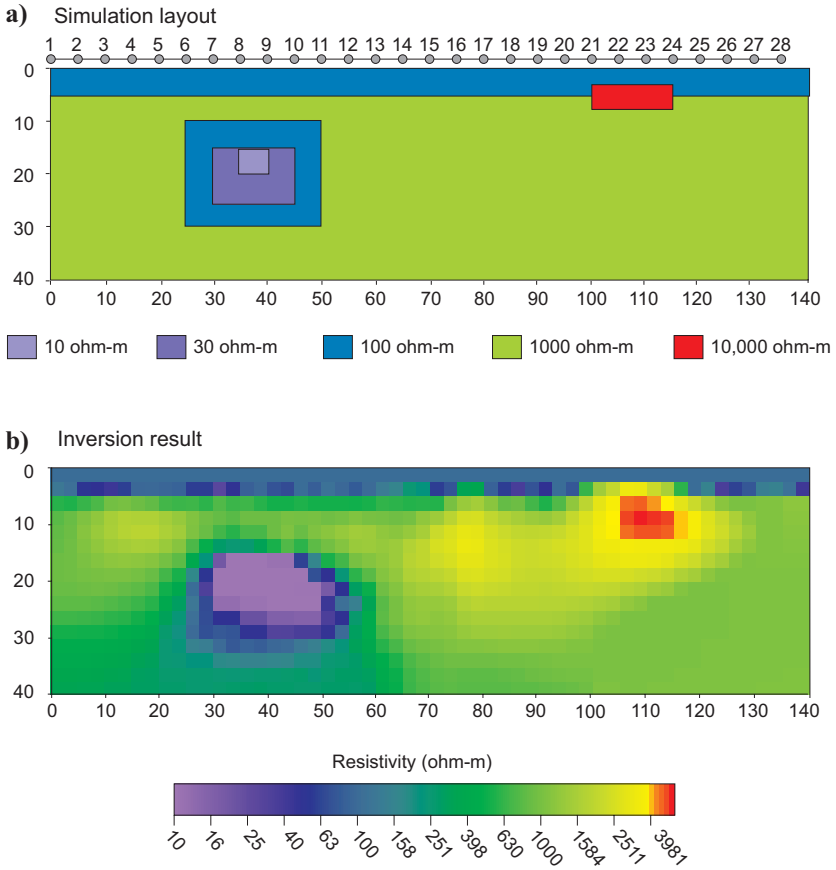

Figure 7. A synthetic numerical modeling and inversion experiment to show the effectiveness of the new data-acquisition strategy. a) This model is identical to the model used in Stummer et al. (2004) for testing optimised real-time experimental design systems. Only 28 electrodes are used, and no noise is added for this experiment. b) The inversion result for data obtained with the proposed configuration is shown. The inversion results of Stummer et al. (2004) for the same model but using optimised measurements (electrode combinations) of 5,740 and 10,310 data points are of very similar quality and appearance to those presented here for the new flexible electrode array. Our results are far superior to those obtained with Wenner, dipole-dipole, and other standard arrays.

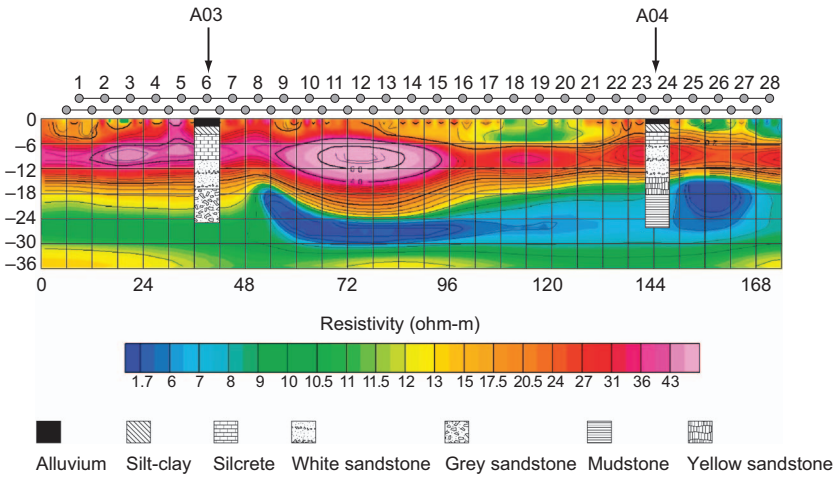

Figure 8. Field example of the prototype system from Coober Pedy, South Australia. The survey used two end-to-end cables laid out on the ground surface at an electrode spacing of 6 m. The cables were then displaced along the line by 3 m and the recording repeated, thus yielding a 168-m-long line sampled every 3 m. The complete set of 10,182 voltage waveforms were then analysed and the data were inverted to produce the model shown. Drillhole results superimposed show that the sandstone is fairly resistive and the mudstone is conductive. The electrical delineation of such subsurface structure is beneficial to opal mining in the area.

with the mudstone in borehole A04. This conductive layer seems to extend further along the profile. The correlation between the resistivity highs and lows and the subsurface variations in the opal-bearing formations is encouraging for future exploration of the area. A possible fault is evident in the resistivity image below station 54 m, where the basal conductive layer is sharply uplifted.

CONCLUSIONS

The resistivity data-collection strategy proposed in this paper is a multichannel and multielectrode, full waveform resistivity acquisition system. This hardware system can be built in any electronics workshop, and the idea of flexible electrode recording is easily implemented in practice. This system allows for large data collection capacity and versatility without the channel sacrifice that occurs with a preselected array. The superior interpretation quality is enabled by the increased data and the monitoring of noise through full waveform display. The hardware is robust, and no electronics need to be installed in the cable. Therefore, it is suitable for 2D or 3D surface or crosshole tomography. It is also well designed for nonconventional resistivity surveys when no traditional electrode configuration can be used. The versatile data acquisition strategy is also robust to noise because no remote electrode is used. The fast acquisition rate means also that this system is well-suited to monitoring applications. The data sets collected with this strategy are suitable for an inversion process involving a large amount of data because the number of voltage values measured using a couple of current electrodes is maximized.

The approach proposed in this paper can be seen as an alternative to optimized resistivity surveying by means of experimental design. A major feature of our approach is to capture all of the electrode combinations subject to having one current electrode in each cable. This is efficient because there is no extra cost in doing this. It is an automatic process because one does not have to make any prior decisions as to what electrode combinations to use.

Further work should be done on the sensitivity of these nontraditional arrays as well as on the influence of the choice for the reference potential electrode location.

REFERENCES

Barker, R., 1981, The offset system of electrical resistivity sounding and its use with a multicore cable: Geophysical Prospecting, **29**, 128–143.

Beresnev, I. A., C. E. Hruby, and C. A. Davis, 2002, The use of multi-electrode resistivity imaging in gravel prospecting: Journal of Applied Geophysics, **49**, 245–254.

Chambers, J., R. Ogilvy, and P. Meldrum, 1999, 3D resistivity imaging of buried oil- and tar-contaminated waste deposits: European Journal of Environmental and Engineering Geophysics, **4**, 3–14.

Dahlin, T., and C. Bernstone, 1997, A roll-along technique for 3D resistivity data acquisition with multi-electrode arrays: Proceedings of the Symposium on the Application of Geophysics to Environmental and Engineering Problems (SAGEEP).

Dahlin, T., and B. Zhou, 2004, A numerical comparison of 2D resitivity imaging with ten electrode arrays: Geophysical Prospecting, **52**, 379–398.

Dahlin, T., and B. Zhou, 2006, Gradient array measurements for multi-channel 2D resistivity imaging: Near Surface Geophysics, **4**, 113–123.

Daily, W., and E. Owen, 1991, Cross-borehole resistivity tomography: Geophysics, **56**, 1228–1235.

Daniels, J. J., 1977, Three-dimensional resistivity and induced-polarization modeling using buried electrodes: Geophysics, **42**, 1006–1019.

Daniels, J. J., 1983, Hole-to-surface resistivity measurements: Geophysics, **48**, 87–97.

Greenhalgh, S. A., B. Zhou, and A. G. Green, 2006, Solutions, algorithms and inter-relations for local minimisation search geophysical inversion: Journal of Geophysics and Engineering, **3**, 101–113.

Griffiths, D. H., J. Turnbull, and A. J. Olayinka, 1990, Two-dimensional resistivity mapping with a computer-controlled array: First Break, **8**, 120–129.

Jackson, P. D., 1981, Focussed electrical resistivity arrays: Some theoretical and practical experiments: Geophysical Prospecting, **29**, 601–626.

Kampke, A., 1999, Focused imaging of electrical resistivity data in archaeological prospecting: Journal of Applied Geophysics, **41**, 215–227.

Li, Y., and D. Oldenburg, 1992, Approximate inverse mappings in DC resistivity problems: Geophysical Journal International, **109**, 343–362.

Loke, M. H., and R. D. Barker, 1996a, Rapid least-squares inversion of apparent resistivity pseudosections using a quasi-Newton method: Geophysical Prospecting, **44**, 131–152.

———, 1996b, Practical techniques for 3D resistivity surveys and data inversion: Geophysical Prospecting, **44**, 499–523.

Loke, M. H., and T. Dahlin, 2002, A comparison of the Gauss-Newton and quasi-Newton methods in resistivity imaging inversion: Journal of Applied Geophysics, **49**, 149–162.

Marescot, L. , S. Palma Lopes, S. Rigobert, J. M. Piau, P. Humbert, R. Lagabrielle, and D. Chapellier, 2004, Forward and inverse resistivity modelling on complex three dimensional structures using the finite element method: Proceedings of the Symposium on the Application of Geophysics to Environmental and Engineering Problems.

Meekes, J. A. C., 1993, Overview of geophysical techniques for groundwater and environmental applications: EAEG, Abstracts of Papers, 55, D041.

Meju, M. A., and M. Montague, 1996, Basis for a flexible low cost automated resistivity data acquisition and analysis system: International Journal of Rock Mechanics: Abstracts, **33**, 264A–265A.

Ogilvy, R., P. Meldrum, and J. Chambers, 1999, Imaging of industrial waste deposits and buried quarry geometry by 3-D resistivity tomography: European Journal of Environmental and Engineering Geophysics, **3**, 103–113.

Park, S. K., and G. P. Van, 1991, Inversion of pole-pole data for 3-D resistivity structure beneath arrays of electrodes: Geophysics, **56**, 951–960.

Roy, K. K., and D. J. Dutta, 1997, Relative performance of focused and unfocused devices in a two-dimensional borehole environment: Journal of Applied Geophysics, **36**, 181–194.

Sasaki, Y., 1992, Resolution of resistivity tomography inferred from numerical simulation: Geophysical Prospecting, **40**, 453–464.

Shima, H., 1992, 2-D and 3-D resistivity imaging reconstruction using crosshole data: Geophysics, **55**, 682–694.

Slater, L., A. M. Binley, W. Daily, and R. Johnson, 2000, Cross-hole electrical imaging of a controlled saline tracer injection: Journal of Applied Geophysics, **44**, 85–102.

Stummer, P., H. Maurer, and A. Green, 2004, Experimental design; electrical resistivity data sets that provide optimum subsurface information: Geophysics, **69**, 120–139.

Stummer, P., H. Maurer, H. Horstmeyer, and A. G. Green, 2002, Optimization of DC resitivity data acquisition: Real-time experimental design and a new multielectrode system: IEEE Transactions on Geosciences and Remote Sensing, **40**, 2727–2735.

Tripp, A. C., G. W. Hohmann, and C. M. Swift, 1984, Two-dimensional resistivity inversion: Geophysics, **49**, 1708–1717.

Xu, B., and M. Noel, 1993, On the completeness of data sets with multi-electrode systems for resistivity surveys: Geophysical Prospecting, **41**, 791–801.

Zhang, J., R. L. Mackie, and T. R. Madden, 1995, 3-D resistivity forward modelling and inversion using conjugate gradients: Geophysics, **60**, 1313–1325.

Zhou, B., and S. A. Greenhalgh, 1999, Explicit expressions and numerical calculations for the Frechet and second derivatives in 2.5-D Helmholtz equation inversion: Geophysical Prospecting, **47**, 443–468.

———, 2000, Crosshole resistivity tomography using different electrode configurations: Geophysical Prospecting, **48**, 887–912.

———, 2002, Rapid 2D/3D crosshole resistivity imaging using the analytic sensitivity function: Geophysics, **67**, 755–765.